Characterisation of Brain Anisotropy using Diffusion MRI

M. M. Correia[1], S. Harding[1], T. A. Carpenter[1], and G. Williams[1]
[1]Wolfson Brain Imaging Centre, Cambridge, United Kingdom

Introduction

It is now well established that the information provided by Diffusion MRI can be very useful in characterising the anisotropy of the brain [1,2]. However, an anisotropy measurement based on the traditional diffusion tensor model [3], such as Fractional Anisotropy (FA) [4], produces significantly low values when there are fibres crossing within the same voxel. This observation led to a recent interest in finding measurements of anisotropy that do not depend on fitting the data to a tensor model (e.g. [5,6]). Here we describe an anisotropy index based on the variance of the diffusion MRI signal.

Methods

If diffusion is isotropic, the measured MRI signal expressed as the radius from the origin as a function of the spherical coordinates (θ,ϕ) has the shape of a perfect sphere. Anisotropic diffusion deviates from this spherical surface in a way that depends on the characteristics of the local diffusion. The deviation of the measured signal from the spherical shape is therefore a measure of anisotropy:

$$SSV = < S^2 > - < S >^2 = \frac{1}{N}\sum_{i=1}^{N} S_i^2 - \left(\frac{1}{N}\sum_{i=1}^{N} S_i\right)^2$$

where N is the number of gradient directions used and S_i is the measured MR signal for each direction. This parameter will be called SSV (Spherical Signal Variance). This method was applied to four data sets of healthy volunteers (20 cm FoV, voxel dimensions 1.5 x 1.5 x 2.0 mm^3). For comparative effects, other measures of anisotropy (FA [4], GA (Generalised Anisotropy) [5] and SDV (Spherical Diffusion Variance) [6]) were also calculated. To better compare these indices of anisotropy, simulations were performed, using typical diffusivity values for cerebral white matter. Both experimental and simulated data were obtained using 63 non-collinear directions and one b-value of 1000 s/mm^2. Simulation data was also used to estimate the minimum number of directions required to estimate SSV accurately.

Results

The results of the simulations show that the ratios FA/SSV and GA/SSV increase as the simulated signal to noise ratio increases, which suggests that SSV is more robust in the presence of noise than these two anisotropy indices. We also notice that these ratios decrease as the simulated anisotropy gets higher, suggesting that SSV images will show a better contrast between regions of high and low anisotropy than FA or GA images. In Figure 1 we present the results obtained for FA, GA, SDV and SSV for one of the datasets analysed. When compared to FA maps, SSV images show a better contrast between regions of high and low anisotropy, as predicted by the simulations. GA images show a better contrast when compared to FA maps, but we can see more detail in the fibre structure in SSV images. In addition, in SSV images the fibre tracks appear to be thicker and brighter, which agrees better with the information we get from structural images, especially in the region of the corpus callosum. Since the variance of the noise is much lower than the variance of the signal within the brain, the noise is not visible in these images. In SDV images the contrast is generally worse and lots of structure detail is lost. The minimum number of directions for robust estimation of SSV is $39 \leq N_{min} \leq 43$.

Normalisation of SSV

SSV can, in theory, assume any value between zero and infinity. While SSV=0 corresponds to perfect isotropy, the upper limit of this parameter is not well defined, which makes it difficult to scale the images in a consistent way – without this, comparison between different subjects is not possible. Normalisation of these images can be achieved by applying a function

$$f(x) = e^{-\sigma / x^2}$$

to the SSV data, where σ is determined by selecting the voxels satisfying the conditions $0.5 \leq FA \leq 0.6$ and $SSV > p \times \max(SSV)$, and using them to find the value of σ that fits better to $FA = e^{-\sigma / SSV^2}$. The reason for this is that FAs in this range correspond to white matter regions of the brain that show the same values of FA for all the datasets analysed. However, there are two voxel populations in an FA image: the noise voxels and the voxels within the brain. But we can use SSV maps to discriminate between the two voxel populations by rejecting the voxels that have a value of SSV lower that a certain percentage p of the maximum value of SSV for each dataset. The optimal value of p was determined by minimising the parameter:

$$\xi(p) = \sum_{i=1}^{N_{voxel}} \left(\frac{SSV_i}{\max(SSV_i)} - \frac{SSV_{norm}(p)_i}{\max(SSV_{norm}(p))} \right)$$

where N_{voxel} is the total number of voxels. Figure 1 shows the results obtained for SSV after normalisation for one of the datasets analysed. The original SSV images and the normalised ones look very similar – they show the same structures with identical contrast.

Conclusions

It has been shown that SSV can be used to characterise the anisotropy in the different regions of the brain, and also that this parameter can be normalised. This method is very promising since it can reveal diffusion anisotropy in situations in which the diffusion tensor formalism fails: SSV images show better contrast between regions of high and low anisotropy and we can see more detail in the fibre structure; we identify the same structures in SSV and FA maps, but in SSV images the fibre tracks appear thicker and brighter, and the noise outside the brain is automatically cleared. In addition, the calculations involved in the determination of SSV are very simple and less computationally intensive than those required to estimate FA or GA.

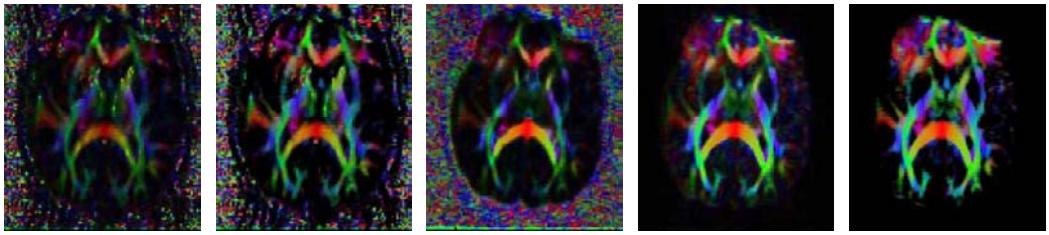

Figure 1 – Anisotropy measurements for one experimental dataset. From the left to the right: FA, GA, SDV, SSV and normalised SSV.

References

[1] PJ Basser, DK Jones. NMR Biomed. 2002, 15:456-467.

[2] D Le Bihan. Nature Reviews Neuroscience 2003, 4:469-480.

[3] PJ Basser *et al*. JMR Series B 1994, 103:247-254.

[4] TE Conturo *et al*. MRM 1996, 35:399-412.

[5] E Ozarslan *et al*. MRM 2005, 53:866-876.

[6] LR Frank. MRM 2001, 45:935-939.